Technical Note

Electroporation of Cells in Microfluidic Droplets

Yihong Zhan, Jun Wang, Ning Bao, and Chang Lu

Anal. Chem., **Article ASAP** • DOI: 10.1021/ac9001172

Electroporation of Cells in Microfluidic Droplets

Yihong Zhan, Jun Wang, Ning Bao, and Chang Lu*

Department of Agricultural and Biological Engineering, Weldon School of Biomedical Engineering, School of Chemical Engineering, Purdue University, West Lafayette, Indiana 47907

Droplet-based microfluidics has raised a lot of interest recently due to its wide applications to screening biological/chemical assays with high throughput. Despite the advances on droplet-based assays involving cells, gene delivery methods that are compatible with the droplet platform have been lacking. In this report, we demonstrate a simple microfluidic device that encapsulates cells into aqueous droplets and then electroporates the encapsulated cells. The electroporation occurs when the cell-containing droplets (in oil) flow through a pair of microelectrodes with a constant voltage established in between. We investigate the parameters and characteristics of the electroporation. We demonstrate delivering enhanced green fluorescent protein (EGFP) plasmid into Chinese hamster ovary (CHO) cells. We envision the application of this technique to high-throughput functional genomics studies based on droplet microfluidics.

Droplet-based microfluidics is a newly emerging field that focuses on transporting and manipulating droplets in microfluidic devices. With droplets serving as monodisperse containers of chemical and biological assays, a variety of applications have been demonstrated ranging from drug discovery, chemical synthesis, and chemical kinetics study, to protein crystallization.[1−3] Droplets have been recently applied to study or process cells with high throughput. Microfluidic droplets that encapsulate cells were used to study gene expression,[4,5] to examine the response of cells to chemical/biological reagents,[6−9] and to process cells for tissue engineering.[10,11] Substantial effort and progress has been made for encapsulating single cells and sorting cell-containing droplets with precision.[12−14]

Gene transfer is the most important tool for studying gene functions. In a typical functional genomics study, a DNA construct is expressed within cells and it directs the overproduction of a gene product or inhibits a function. This is typically followed by a variety of functional assays. Electroporation is a physical tool that is based on applying external electric field to breach the cell membrane for gene transfer. Electroporation as a technique for gene delivery and cell lysis has been successfully adapted in a number of microfluidic devices.[15−23] Although the application of pulses to cell-encapsulating droplets was proposed previously, no data on cell permeabilization and molecule delivery were provided.[24] Applying electroporation to cells in droplets will potentially allow high-throughput functional screening of genes carried out on the platform of droplet microfluidics.

In here we report a simple microfluidic device for electroporating cells that are encapsulated in droplets. Cells are first encapsulated into aqueous droplets in oil, and then the cell-containing droplets in oil flow to downstream where a pair of surface microelectrodes are located. With a constant voltage between the electrodes, electric current runs through the conductive buffer droplets to electroporate cells inside when the droplets flow through the channel. The duration and intensity of the electroporation are defined by the velocity (1.38−8.86 m/min) and dimensions of the droplets (60−386 μm in the length), the distance between the electrodes (~20 μm), and the voltage applied (5−9 V). We demonstrate delivery of a plasmid vector coding enhanced

* To whom correspondence should be addressed. E-mail: changlu@purdue.edu. Phone: 765-494-1188. Fax: 765-496-1115.

(1) Teh, S. Y.; Lin, R.; Hung, L. H.; Lee, A. P. *Lab Chip* **2008**, *8*, 198–220.
(2) Huebner, A.; Sharma, S.; Srisa-Art, M.; Hollfelder, F.; Edel, J. B.; Demello, A. J. *Lab Chip* **2008**, *8*, 1244–1254.
(3) Gunther, A.; Jensen, K. F. *Lab Chip* **2006**, *6*, 1487–1503.
(4) Clausell-Tormos, J.; Lieber, D.; Baret, J. C.; El-Harrak, A.; Miller, O. J.; Frenz, L.; Blouwolff, J.; Humphry, K. J.; Koster, S.; Duan, H.; Holtze, C.; Weitz, D. A.; Griffiths, A. D.; Merten, C. A. *Chem. Biol.* **2008**, *15*, 427–437.
(5) Huebner, A.; Srisa-Art, M.; Holt, D.; Abell, C.; Hollfelder, F.; deMello, A. J.; Edel, J. B. *Chem. Commun.* **2007**, 1218–1220.
(6) Boedicker, J. Q.; Li, L.; Kline, T. R.; Ismagilov, R. F. *Lab Chip* **2008**, *8*, 1265–1272.
(7) Kline, T. R.; Runyon, M. K.; Pothiawala, M.; Ismagilov, R. F. *Anal. Chem.* **2008**, *80*, 6190–6197.
(8) Huebner, A.; Olguin, L. F.; Bratton, D.; Whyte, G.; Huck, W. T.; de Mello, A. J.; Edel, J. B.; Abell, C.; Hollfelder, F. *Anal. Chem.* **2008**, *80*, 3890–3896.
(9) He, M. Y.; Edgar, J. S.; Jeffries, G. D. M.; Lorenz, R. M.; Shelby, J. P.; Chiu, D. T. *Anal. Chem.* **2005**, *77*, 1539–1544.
(10) Demirci, U.; Montesano, G. *Lab Chip* **2007**, *7*, 1428–1433.
(11) Demirci, U.; Montesano, G. *Lab Chip* **2007**, *7*, 1139–1145.
(12) Edd, J. F.; Di Carlo, D.; Humphry, K. J.; Koster, S.; Irimia, D.; Weitz, D. A.; Toner, M. *Lab Chip* **2008**, *8*, 1262–1264.
(13) Koster, S.; Angile, F. E.; Duan, H.; Agresti, J. J.; Wintner, A.; Schmitz, C.; Rowat, A. C.; Merten, C. A.; Pisignano, D.; Griffiths, A. D.; Weitz, D. A. *Lab Chip* **2008**, *8*, 1110–1115.
(14) Chabert, M.; Viovy, J. L. *Proc. Natl. Acad. Sci. U.S.A.* **2008**, *105*, 3191–3196.
(15) Huang, Y.; Rubinsky, B. *Sens. Actuators, A* **2003**, *104*, 205–212.
(16) Fei, Z.; Wang, S.; Xie, Y.; Henslee, B. E.; Koh, C. G.; Lee, L. J. *Anal. Chem.* **2007**, *79*, 5719–5722.
(17) Kim, S. K.; Kim, J. H.; Kim, K. P.; Chung, T. D. *Anal. Chem.* **2007**, *79*, 7761–7766.
(18) Wang, H. Y.; Lu, C. *Biotechnol. Bioeng.* **2008**, *100*, 579–586.
(19) Valero, A.; Post, J. N.; van Nieuwkasteele, J. W.; Ter Braak, P. M.; Kruijer, W.; van den Berg, A. *Lab Chip* **2008**, *8*, 62–67.
(20) McClain, M. A.; Culbertson, C. T.; Jacobson, S. C.; Allbritton, N. L.; Sims, C. E.; Ramsey, J. M. *Anal. Chem.* **2003**, *75*, 5646–5655.
(21) Lu, H.; Schmidt, M. A.; Jensen, K. F. *Lab Chip* **2005**, *5*, 23–29.
(22) Khine, M.; Lau, A.; Ionescu-Zanetti, C.; Seo, J.; Lee, L. P. *Lab Chip* **2005**, *5*, 38–43.
(23) Wang, H. Y.; Lu, C. *Chem. Commun.* **2006**, 3528–3530.
(24) Luo, C.; Yang, X.; Fu, Q.; Sun, M.; Ouyang, Q.; Chen, Y.; Ji, H. *Electrophoresis* **2006**, *27*, 1977–1983.

10.1021/ac9001172 CCC: $40.75

green fluorescent protein (EGFP) into Chinese hamster ovary (CHO) cells.

EXPERIMENTAL SECTION

Microfluidic Device Fabrication. Microfluidic devices were fabricated based on poly(dimethylsiloxane) (PDMS) using standard soft lithography method.[25] The microscale patterns were first created using computer-aided design software (FreeHand MX, Macromedia, San Francisco, CA) and then printed out on a high-resolution (5080 dpi) transparency. SU-8 2025 negative photoresist (Microchem Corp., Newton, MA) was spun on a 3 in. silicon wafer to create a layer of 33 μm thickness. The coated wafer was prebaked before it was exposed to UV light and developed. PDMS prepolymer mixture consisting of monomer (A) and curing agent (B) (General Electric Silicones RTV 615, MG Chemicals, Toronto, ON, Canada) was cast on the master and heated at 80 °C for 1 h before it was peeled off and punched to create inlets and outlets. For the fabrication of surface microelectrodes, a gold layer with a thickness of 150 nm was deposited onto precleaned glass slides using an E-beam evaporator (Temescal FC-1800, Fairfield, CA) with an adhesion layer of titanium (20 nm thick) between the glass and the gold. Positive photoresist AZ 9260 (Clariant Corp., Somerville, NJ) was coated and patterned on the metal/glass substrate before the electrodes were fabricated by wet etching. The photoresist was removed by acetone to yield glass slides with surface microelectrodes. The PDMS chip and the electrode/glass substrate were aligned and bonded together after both surfaces were oxidized in a plasma cleaner (Harrick Plasma, Ithaca, NY). To attain strong bonding, the device was baked at 80 °C for additional 30 min before use. The device was finally treated with 1,1,2,2-tetrahydrooctyl-1-trichlorosilane (United Chemical Technologies, Bristol, PA) vapor under house vacuum for 2 h to render the channel surface hydrophobic.

Plasmid Preparation and Cell Culture. A plasmid vector pEGFP-C1 (Clontech, Palo Alto, CA), 4.7 Kb and coding EGFP, was propagated in *Escherichia coli*, extracted, and purified using the QIAfilter Plasmid Giga kit (Qiagen, Valencia, CA). The plasmid was dissolved in Tris−EDTA buffer and stored at −20 °C until use. The reporter gene expression was used to indicate successful gene transfection. Chinese hamster ovary (CHO-K1) cells were grown at 37 °C with 5% CO_2 in Dulbecco's modified Eagle's medium (DMEM, Mediatech, Inc., Herndon, VA) supplemented with 10% (v/v) fetal bovine serum (Sigma, St. Louis, MO) and penicillin (100 μg/mL, Sigma, St. Louis, MO). The cells were trypsinized and diluted at a ratio of 1:5−1:8 every 2 days to maintain the cells in the exponential growth phase. For transfection, cells were centrifuged at 260*g* for 5 min and resuspended in an electroporation buffer (8 mM Na_2HPO_4, 2 mM KH_2PO_4, and 250 mM sucrose, pH = 7.2) at a concentration of 3×10^7 cells/mL with the plasmid concentration at 100 μg/mL. To prevent clogging, the electroporation buffer was prefiltered by 0.2 μm filter.

Microchip Operation and Cell Transfection. A schematic of the droplet-based electroporation device is shown in Figure 1. Droplets were produced in the T-junction channel using the electroporation buffer as the disperse phase and hexadecane

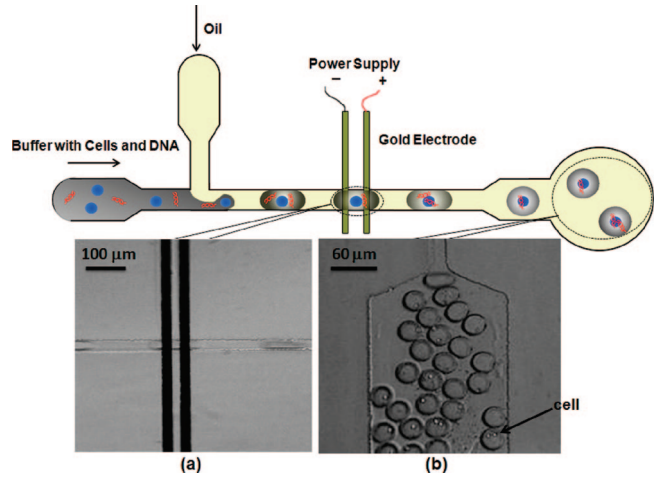

Figure 1. Layout and performance of the droplet-based microfluidic electroporation device. The depth of the channel was ~33 μm. Inset images illustrate the processing of the droplets at different sections of the device. (a) Cell-containing droplets rapidly flow through the two microelectrodes on the substrate (each electrode was 25 μm wide, and the distance between the two electrodes was 20 μm). (b) The droplets with encapsulated cells after electroporation at the exit of the device.

(viscosity $\eta = 3.4 \times 10^{-3}$ Pa s; density = 0.773 g/mL, Sigma, St. Louis, MO) as the continuous phase. An amount of 5 wt % of surfactant Span80 (Sigma, St. Louis, MO) was added to hexadecane to prevent spontaneous drop coalescence. Droplets of different sizes were produced by adjusting the flow rates of the oil and the buffer using syringe pumps (PHD infusion pump, Harvard Apparatus, MA). Droplet movement was recorded by a CCD camera (ORCA-285, Hamamatsu, Bridgewater, NJ) at a frame rate of 32 Hz. A dc power supply (1AA12P30, Ultravolt, Ronkonkoma, NY) provided constant dc voltage. Electrical current was first amplified by a low-noise current preamplifier (SR570, Standard Research System, Sunnyvale, CA) and then converted to voltage and digitalized by the PCI-6254 data acquisition card (National Instrument, Austin, TX). The digitalized signal was recorded by a LabView program at the frequency of 10^5 Hz. For droplet-based cell transfection, droplets with a length of 92 μm were generated with cells encapsulated inside. The cells were delivered into the microfluidic device by a syringe pump. A magnetic bar was stirring inside the syringe to prevent cells from settling down. After electroporation, emulsion solution with electroporated cells was collected from the outlet reservoir and put in a centrifuge tube. The tube was centrifuged at 300*g* for 5 min after settling for 30 min. The upper oil layer was carefully removed by a pipet, and 150 μL of fresh cell culture medium was then added to the aqueous layer before the tube was centrifuged again and the oil layer was removed one more time. Finally, the cell suspension was transferred into a 96 well plate with fresh DMEM medium. In order to get proper cell confluence rate, the cells were cultured for 6 days with medium being changed every 2 days before phase contrast and fluorescent images were taken. The epifluorescence excitation was provided by a 100 W mercury lamp, together with bright-field illumination. The excitation and emission from cells were filtered by a fluorescence filter cube (Exciter HQ 480/40, emitter HQ535/50, and beam splitter Q505lp, ChromaTechnology, Rockingham, VT).

(25) Duffy, D. C.; McDonald, J. C.; Schueller, O. J. A.; Whitesides, G. M. *Anal. Chem.* **1998**, *70*, 4974–4984.

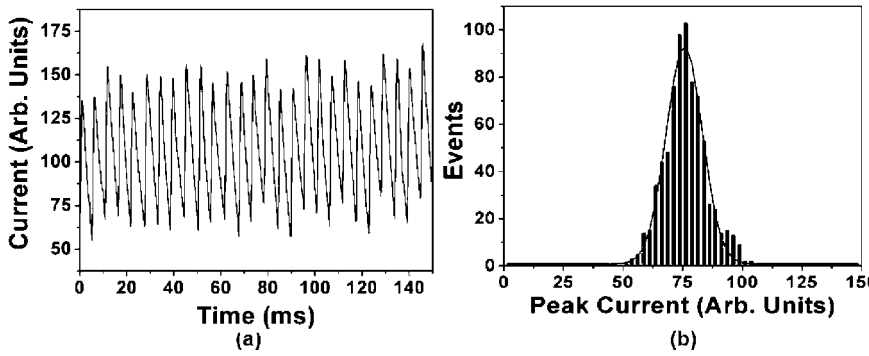

Figure 2. (a) Current variation over time caused by flowing droplets while the voltage between the electrodes was 7.2 V. The flow rates of the electroporation buffer and the oil were 1 and 3 μL/min, respectively. (b) Histogram of the peak currents fitted with a normal distribution. The current data were taken with the same conditions as in panel a within 4.5 s. The peak current refers to the height of a current peak.

We noticed that there was damage to the electrodes when a voltage of >7 V was applied for an extended period (>5 min). It was presumably due to etching of the adhesion layer. Such problem can be potentially avoided by using electrode materials that do not require adhesion layer (e.g., indium tin oxide).

Cell Viability. SYTOX green nucleic acid stain (MW ~600, 504/523 nm, Invitrogen, Carlsbad, CA) was used to test the cell viability. Cells in droplets were electroporated and collected to a 384 well plate. The cell samples were centrifuged and pipetted to remove oil as described above. SYTOX green was added to the cell sample 1 h after the electroporation to generate a final concentration of 1 μM. Both phase contrast and fluorescent images of cells were taken at 10 different locations for each sample to obtain the percentages of nonfluorescent cells among the total population which was defined as the cell viability. Every data point was based on three runs.

RESULTS AND DISCUSSION

The layout of the droplet-based electroporation device is shown in Figure 1. A simple T-junction channel was used to produce droplets of monodispersity. Cells in the aqueous buffer solution (with the plasmid DNA) were encapsulated into the droplets at the junction. As shown by the inset image Figure 1b, most droplets encapsulated one or two cells and a fraction of the droplets were empty. There was a constant voltage established across a pair of gold microelectrodes on the glass substrate in the downstream during the electroporation. The droplets with cells continuously flowed through the microelectrode pair (Figure 1a). Because the oil phase was nonconductive, each flowing buffer droplet experienced a field intensity variation that was equivalent to a pulse for the transit time that the two electrodes were connected by the droplet. Such duration was determined by the distance between the two electrodes and the velocity and length of the droplet.

Figure 2a shows the current variation while the droplets flowed through the electrodes with a constant voltage of 7.2 V applied between the electrodes and the flow rates of the buffer and oil being 1 and 3 μL/min, respectively. Figure 2b shows the histogram of the peak currents (the peak current refers to the height of a current peak) during a period of 4.5 s. The histogram matches a normal distribution that has a standard deviation of 10% of the average. Some of the deviation might be contributed by small variation in the current baseline.

We examined whether the current peaks corresponded to the passage of the buffer droplets. We varied the flow rate of the oil,

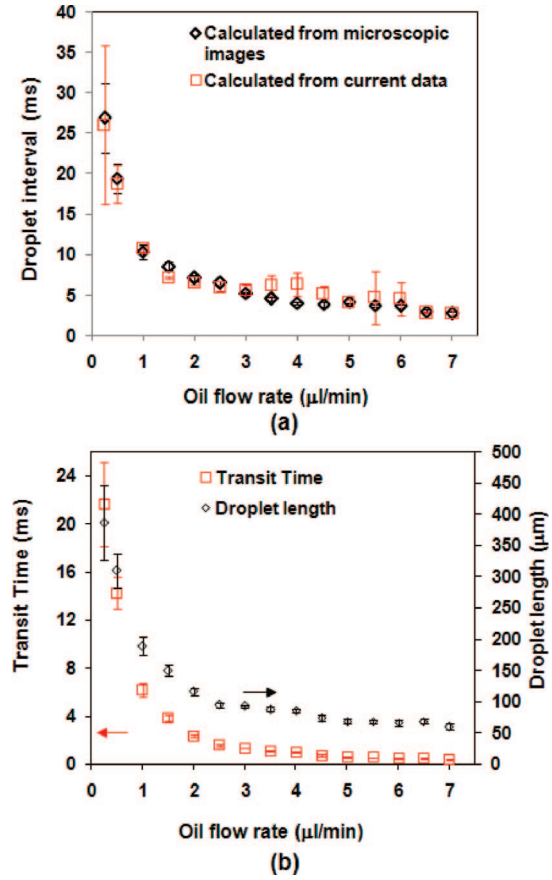

Figure 3. (a) Comparison of droplet intervals (the time lapsed between droplets) calculated based on microscopic images and those obtained from the current data. The buffer flow rate was kept at 1 μL/min while the oil flow rate changed. (b) The electroporation zone transit time and the droplet length with different oil flow rates. The buffer flow rate was kept at 1 μL/min. The electroporation zone transit time refers to the duration that the two electrodes are connected by a flowing droplet.

and the variation in the oil flow rate led to variation in the length and spacing of the aqueous droplets. In Figure 3a, we used two methods to calculate the intervals (in milliseconds) between the droplets. In the first method, we assumed that the current data accurately reflected the flowing-through of the droplets and the intervals between the current peaks in the time-lapsed current data were equal to the intervals between the droplets. In the second method, we were able to calculate the intervals by knowing

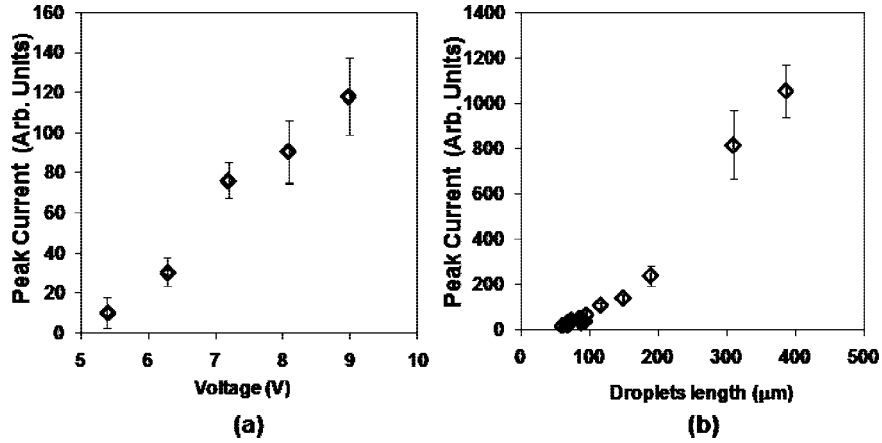

Figure 4. (a) Variation in the peak current with different voltages. The droplets were generated by having the buffer flow rate at 1 μL/min and the oil flow rate at 3 μL/min. (b) The variation in the peak current with different lengths of droplets. The buffer flow rate was constant at 1 μL/min, and the oil flow rate was varied from 7 to 0.25 μL/min.

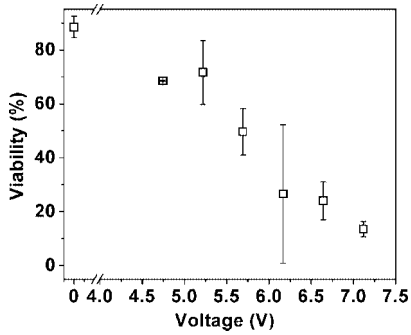

Figure 5. Cell viability after droplet-based electroporation under different voltages. The droplets were generated by having the buffer flow rate at 1 μL/min and the oil flow rate at 3 μL/min. The viability is defined as the percentage of viable cells in the cell population.

the velocity of the droplets (calculated from the volumetric flow rate and the cross-sectional area of the channel) and the distance between the droplets (obtained from microscopic images of the droplet flow). Figure 3a shows that the two sets of results are very consistent over a wide range of flow rates. This indicates that the peaks in the current accurately reflected the electrical shocks that the flowing droplets experienced. Figure 3b shows that the length of the droplets we produced ranged from 60 to 386 μm and the electroporation zone transit time (the duration for a droplet to be electrically connected to the electrode pair) ranged from 0.37 to 21.6 ms. The droplets of different sizes were produced by maintaining the buffer flow rate at 1 μL/min and varying the oil flow rate from 7 to 0.25 μL/min. This duration range is appropriate for electroporation of mammalian cells.

Figure 4a shows that the peak current increased with the applied voltage, while the size of the droplets was kept constant. This indicates that the buffer droplets were conductors under our experimental conditions. The ionic buffer droplets here behaved much more like perfect conductors than water droplets which are known to deviate from conductors in terms of their charging process.[26] Figure 4b shows that the peak current increased with the droplet length when the voltage was kept constant. The droplet lengths in this study (from 60 to 386 μm) were all substantially larger than the distance between the two electrodes (~20 μm).

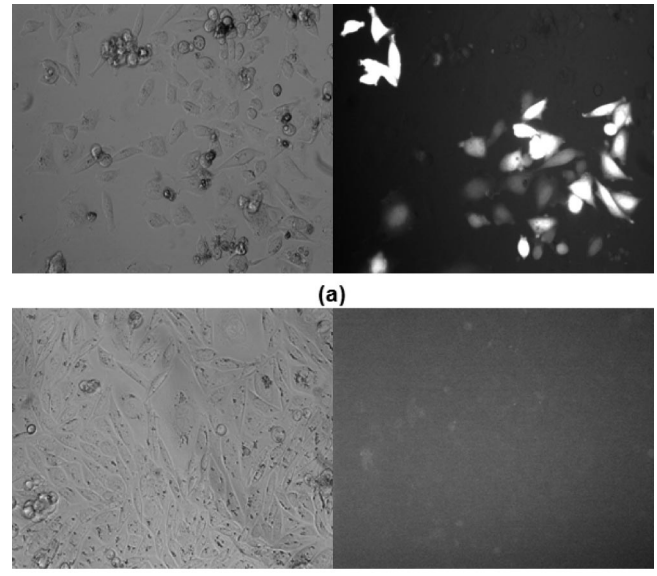

Figure 6. Transfection of CHO cells using droplet-based electroporation. The phase contrast image is on the left, and the fluorescence image of the same cells is on the right. (a) A fraction of the cells showing expression of pEGFP-C1 vector. Cells were electroporated at the voltage of 5.8 V with the flow rates of the buffer and oil at 1 and 3 μL/min, respectively. The percentage of transfected cells in the image is not representative of the entire population. (b) A control sample with cells processed in the same fashion as above without the electricity on. No transfection occurred.

The nonlinearity in these curves is possibly related to the deformation of the droplets in the electric field and the interaction between the oil and the hydrophobic gold electrodes. We modeled the electric field inside the droplet (Supporting Information Figures S1 and S2).[27] The data show that the field intensity on the cell membrane is highly dependent on the location of the cell (relative to those of the two electrodes) at the moment when the droplet is in contact with both electrodes. For example, when the voltage across the electrodes is 5 V, the field intensity on the membrane ranges from hundreds to thousands of volts per centimeter (Supporting Information Table S1).

(26) Jung, Y. M.; Oh, H. C.; Kang, I. S. *J. Colloid Interface Sci.* **2008**, *322*, 617–623.

(27) Gawad, S.; Schild, L.; Renaud, P. H. *Lab Chip* **2001**, *1*, 76–82.

We tested the cell viability after the droplet-based electroporation (Figure 5). There was a small percentage of cell death (11%) when the electricity was not applied, indicating that the contact with oil compromised cell viability. The percentage of viable cells dropped with increasing voltage from ~68% with 4.7 V applied to ~14% with 7.1 V.

We tested the delivery of a plasmid vector coding EGFP into CHO cells based on electroporation in droplets. Figure 6a shows the phase contrast and fluorescence images of CHO cells after the droplet-based electroporation and culture. Cells were electroporated with the applied voltage of 5.8 V and the electroporation zone transit time of 1.8 ms. A fraction of the cells were transfected (~11%) with the plasmid vector. In comparison, Figure 6b shows that cells processed in droplets without electricity did not have gene expression but had high density due to less cell death. Tiny droplets of oil can be observed in some of the cells in both cases. The transfection efficiency here was likely affected by many factors including the electrical parameters, the dimensions of the droplets, and the location of the encapsulated cell(s) during the electroporation. The optimization of these parameters will likely improve the transfection efficiency.

CONCLUSIONS

In this study, a simple microfluidic device and a common dc power were used to conduct electroporation of cells encapsulated in droplets. Such technique allows delivery of genes into cells within the confined space of a microscale droplet. No pulse generator was required. This technique paves the way to conduct functional genomics studies by taking advantage of the high throughput of droplet microfluidics.

ACKNOWLEDGMENT

This research was supported by the Wallace H. Coulter Foundation and NSF Grant CBET-0747105.

SUPPORTING INFORMATION AVAILABLE

Additional information as noted in text. This material is available free of charge via the Internet at http://pubs.acs.org.

Received for review January 17, 2009. Accepted January 22, 2009.

AC9001172